RESEARCH PAPER

Acta Neurobiol Exp 2020, 80: 57–65
DOI: 10.21307/ane-2020-006

Hindbrain metabolic deficiency regulates ventromedial hypothalamic nucleus glycogen metabolism and glucose-regulatory signaling

Karen P. Briski* and Santosh K. Mandal

School of Basic Pharmaceutical and Toxicological Sciences, College of Pharmacy, University of Louisiana at Monroe, United States,
** Email: briski@ulm.edu*

The catecholamine norepinephrine (NE) links hindbrain metabolic-sensory neurons with downstream gluco-regulatory loci, including the ventromedial hypothalamic nucleus (VMN). Exogenous NE up-regulates VMN expression of glutamate decarboxylase (GAD), biomarker for the gluco-inhibitory transmitter γ-aminobutryic acid (GABA). Brain glycogen phosphorylase (GP)-muscle (GPmm) and -brain (GPbb) variants are stimulated *in vitro* by NE or energy deficiency, respectively. Current research investigated whether lactoprivic-driven VMN NE signaling regulates GABA and if VMN GPmm and GPbb profiles react differently to that deficit cue. Male rats were pretreated by caudal fourth ventricle delivery of the selective catecholamine neurotoxin 6-hydroxydopamine (6OHDA) ahead of the monocarboxylate transporter inhibitor alpha-cyano-4-hydroxycinnamic acid (4CIN). Micropunch-dissected VMN tissue was analyzed by Western blot and ELISA to assess NE-dependent 4CIN regulation of GAD and GP variant protein expression and NE activity. 4CIN caused 6OHDA-reversible augmentation of VMN NE content and plasma glucose and counter-regulatory hormone levels. 6OHDA stimulated basal VMN GAD expression, but prevented 4CIN stimulation of this profile. Neurotoxin inhibited or increased baseline VMN GPmm and GPbb levels, respectively, in non-4CIN-injected rats. 6OHDA deterred 4CIN inhibition of GPmm, but did not prevent drug stimulation of GPbb. Results affirm hindbrain lactoprivic regulation of glucostasis. Hindbrain NE exerts opposite effects on VMN GABA transmission during hindbrain lactostasis *vs.* -privation. VMN norepinephrine- *vs.* energy-sensitive GP variants are subject to dissimilar NE regulation during energy homeostasis, and respond differently to hindbrain lactoprivation.

Keywords: 6-hydroxydopamine, alpha-cyano-4-hydroxycinnamic acid, glutamate decarboxylase$_{65/67}$, glycogen phosphorylase-muscle type, glycogen phosphorylase-brain type

INTRODUCTION

The ventromedial hypothalamic nucleus (VMN) utilizes metabolic sensory information in the form of nutrient, endocrine, and neurochemical cues to direct glucose counter-regulatory motor functions (Watts and Donovan, 2010; 2014). Specialized energy substrate-sensitive neurons in the VMN provide a dynamic cellular energy readout by augmenting ('fuel-inhibited') or decreasing ('fuel-excited') synaptic firing as oxidizable fuel levels dwindle (Oomura et al., 1969; Silver and Erecinska, 1998). Detection of neuro-energetic deficiency within the mediobasal hypothalamus (MBH), which contains the VMN as well as arcuate and tuberal hypothalamic nuclei, is critical for optimal contra-regulatory endocrine and hepatic gluconeogenic responses to hypoglycemia (Borg et al., 1997; 2003). The hypoglycemia-sensitive glucose-inhibitory neurotransmitter γ-aminobutyric acid (GABA) acts within the MBH to control counter-regulation by diminishing glucagon and epinephrine secretory responses to hypoglycemia (Chan et al., 2006).

The VMN and other hypothalamic glucose-regulatory loci receive vital metabolic sensory input

Received 5 September 2019, accepted 4 December 2019

from hindbrain energy sensors in the form of norepinephrine (NE) signaling. Dorsal vagal complex (DVC) A2 noradrenergic neurons are a likely source of such communication as these cells express hypoglycemia-sensitive metabolic sensory biomarkers, e.g., glucokinase, K_{ATP}, and 5'-AMP-activated protein kinase (AMPK) (Briski et al., 2009; Cherian and Briski, 2011). The oxidizable glycolytic end-product L-lactate is monitored in the hindbrain as a critical metabolic variable. The astrocyte-neuron lactate shuttle hypothesis posits that astrocyte lactate trafficking sustains mitochondrial energy production in neurons (Broer et al., 1997; Pellerin et al., 1998; Magistretti et al., 1993). Pharmacological induction of lactoprivation within the DVC, involving inhibition of local monocarboxylate transporter function, is a potent stimulus for hyperglycemia (Patil and Briski, 2005). During hypoglycemia, DVC lactate deficiency activates A2 neurons (Patil and Briski, 2005) and increases hypothalamic NE activity (Shrestha et al., 2014). Hypoglycemic patterns of NE input to the MBH regulate GABA release (Beverly et al., 2000; 2001). Our recent studies affirm a positive causal relationship between NE and VMN GABA as site-targeted delivery of exogenous NE up-regulates the GABA marker protein glutamate decarboxylase$_{65/67}$ ($GAD_{65/67}$) (Ibrahim et al., 2019). Current research investigated the hypothesis that metabolic deficit-propelled NE input to the VMN stimulates GABA signaling. Here, groups of adult male rats were injected into the caudal fourth ventricle (CV4) with the monocarboxylate transporter inhibitor alpha-cyano-4-hydroxycinnamic acid (4CIN) or vehicle alone (Patil and Briski, 2005). Micropunch-dissected VMN tissue was analyzed by Western blotting and ELISA methods to determine 4CIN effects on VMN $GAD_{65/67}$ protein expression and NE activity, respectively. A subset of subjects in each treatment group were pretreated by intra-CV4 delivery of the selective catecholamine neurotoxin 6-hydroxydopamine (6OHDA) (Gujar et al., 2013; Tamrakar et al., 2015; Alhamami et al., 2018) to verify the role of DVC NE in hindbrain lactoprivic regulation of VMN $GAD_{65/67}$.

The role of hindbrain NE in regulation of hypothalamic glycogen energy reserve mobilization is unclear. Brain glycogenolysis, which is catalyzed by glycogen phosphorylase (GP) enzyme activity, increases under circumstances of insufficient energy supply *vs.* demand, e.g., seizure, sleep deprivation, and hypoglycemia (Gruetter, 2003; Brown, 2004) to liberate glucosyl units for conversion to L-lactate (Belanger et al., 2011; Stobart and Anderson, 2013). Multiple GP isoforms are expressed in brain, including muscle- (GPmm) and brain- (GPbb) types, which differ with respect to cell-type localization and regulation by phosphorylation and AMP (Nadeau et al., 2018). GPmm and -bb are both expressed in astrocytes, whereas GPbb occurs exclusively in neurons. Phosphorylation elicits complete *vs.* partial activation of GPmm or GPbb, whereas GPbb exhibits greater affinity for and sensitivity to AMP activation relative to GPmm, and requires AMP binding for optimal enzyme function and Km. Cortical astrocyte cell culture models show that NE is a potent stimulus for glial glycogenolysis (Fillenz et al., 1999; Dong et al., 2012). We reported that VMN astrocytes express NE-sensitive alpha$_1$ (α_1), alpha$_2$ (α_2) and beta$_1$ (β_1) adrenergic receptor (AR) proteins, and that NE inhibits net VMN GP content (Ibrahim et al., 2019). Available *in vitro* studies indicate that GPmm mediates noradrenergic augmentation of glycogenolysis (Müller et al., 2015), but the role of NE in physiological regulation of brain GPmm *in vivo* remains unclear. Cell energy deficits boost GPbb expression *in vitro* (Nadeau et al., 2018). Our work shows that exogenous NE causes coincident up-regulation of VMN GPbb and $GAD_{65/67}$, and that the latter response is abolished by interruption of astrocyte substrate fuel provision (Mahmood et al., 2019). These findings imply that NE may stimulate GABAergic transmission by enhancing glycogen-derived substrate fuel supply, but VMN GPbb sensitivity to noradrenergic metabolic deficit signaling *in vivo* has not been investigated. The present project addressed the premise that hindbrain NE imposes differential control of VMN GPmm *vs.* GPbb protein expression during energy homeostasis, and that lactoprivic driven-NE input elicits dissimilar adjustments in these GP variant profiles.

METHODS

Animals and experimental design

Adult male Sprague-Dawley rats (3–4 months of age) were maintained under a 14 h light : 10 h dark lighting schedule (lights on at 05.00 h), and allowed free access to standard laboratory rat chow (Harlan Teklad LM-485; Harlan Industries, Madison, WI) and tap water. Animals were accustomed to daily handling for a minimum of one week before experimentation. All protocols were conducted in accordance with NIH guidelines for care and use of laboratory animals, under ULM Institutional Animal Care and Use Committee approval. Rats were divided into four treatment groups (n=4/group). On study day 1, animals were anesthetized with ketamine/xylazine (0.1mL/100 g bw ip, 90 mg ketamine: 10 mg xylazine/mL; Butler Schein Inc., Melville, NY), and implanted with a 26-gauge stainless steel cannula (prod no. C315G/

SPC; Plastics One, Inc., Roanoke, VA) aimed at the caudal fourth ventricle (CV4) (Briski and Shrestha, 2016). After surgery, rats were injected subcutaneously (sc) with ketoprofen (1 mg/kg bw) and intramuscularly with enrofloxacin (10 mg/0.1 mL), treated by topical application of 0.25% bupivacaine to closed incisions, then transferred to individual cages. At 9:00 h on days 7 and 9, groups 1 (n=4) and 3 (n=4) were injected into the CV4 with vehicle (v), e.g., sterile apyrogenic water containing 0.2% ascorbic acid, while groups 2 (n=4) and 4 (n=4) rats received 6-hydroxydopamine (6OHDA; 75 ug/1.0 µL (Gujar et al., 2014; Tamrakar et al., 2015; Alhamami et al., 2018). Beginning at 9:00 h on day 10, animals in groups 1 and 2 were infused into CV4 with vehicle (60% DMSO : 40% 0.9% NaCl; 2.0 µL), over a 30 min period using a 33-gauge internal injection cannula (prod. no. C315I/SPC; Plastics One). At the same time, rats in groups 3 and 4 were treated with 4-CIN (75.0 ug/2.0 µL (Patil and Briski, 2005). Animals were sacrificed at 11:00 h on day 10 for blood and brain tissue collection. Dissected brains were immediately snap-frozen in liquid nitrogen-cooled isopentane and stored in -80°C. Plasma was stored at -20°C.

Western blot analysis of VMN glycogen enzyme protein expression

Forebrains were cut into consecutive 200 µm - thick frozen sections through the VMN (-1.78 to -3.25 mm). Calibrated hollow punch tools (prod. no. 57401; Stoelting; Kiel, WI) were used to bilaterally dissect VMN tissue for immunoblotting (right-side VMN punches were collected into lysis buffer consisting of 2.0% sodium dodecyl sulfate, 0.05 M dithiothreitol, 10.0% glycerol, 1.0 mM EDTA, 60 mM Tris-HCl, pH 7.2) or for NE ELISA (left-side VMN punches were collected into 0.01 N HCl supplemented with 1.0 mM EDTA, 4.0 mM sodium metabisulfite). For each protein of interest, heat-denatured tissue aliquots from individual subjects were combined within each treatment group to create triplicate pools ahead of separation in Bio-Rad TGX 10–12% Stain-Free gels (Shakya et al., 2018). After electrophoresis, gels were activated (1 min) by UV light in a Bio-Rad ChemiDoc MP Imaging System (prod. no. 17001395; Hercules, CA) prior to overnight protein transblotting (30 V; 4°C; Towbin buffer) to 0.45-µm PVDF-Plus membranes (prod. no. PV4HY00010; ThermoFisherScientific, Waltham, MA). Membranes were blocked with Tris-buffer saline (TBS), pH 7.4), containing 0.1% Tween-20 and 2.0% bovine serum albumin prior to primary antibody incubation at 4°C for 24 - 36 hours. Proteins of interest were probed with antisera raised in rabbit against glycogen synthase (GS; prod. no. 3893S, 1:2,000; Cell Signaling Technology, Danvers, MA), GPmm (1:2,000; prod. no. NBP2-16689; Novus Biologicals, Littleton, CO), GPbb (prod. no. NBP1-32799, 1:2,000; Novus Biol.), or $GAD_{65/67}$ (1:10,000; prod. no. ABN904; MilliporeSigma, Burlington, MA), as described (Ali et al., 2019; Briski and Mandal, 2019; Napit et al., 2019). Membranes were incubated for 1 h with a peroxidase-conjugated goat anti-rabbit (NEF812001EA, 1:5,000; PerkinElmer, Waltham, MA) secondary antiserum prior to exposure to Supersignal West Femto maximum sensitivity chemiluminescent substrate (prod. no. 34096; ThermoFisherScientific). Membrane buffer washes and antibody incubations were carried out by Freedom Rocker™ Blotlbot® automation (Next Advance, Inc., Troy NY). Protein band chemiluminescence optical density (O.D.) values were obtained in the ChemiDoc MP system, and normalized to individual-lane total protein using Imagelab software (Image Lab™ 6.0.0; BioRad). Precision plus protein molecular weight dual color standards (prod. no. 161-0374; Bio-Rad) were included in each Western blot analysis.

For each animal, micropunched VMN tissue was analyzed for NE content using Noradrenaline Research ELISA™ kit reagents (Labor Diagnostika Nord GmbH & Co KG, Nordhorn, Germany), as reported (Shrestha et al., 2014).

Western blot analysis of DVC dopamine--beta-hydroxylase (DβH) protein expression

DVC A2 area tissue was bilaterally micropunch-dissected from serial 100 µm-thick frozen sections cut between -14.36 and -14.86 mm posterior to bregma. Triplicate tissue lysate pools from each treatment group were analyzed by Stain-Free Western blotting, as described above, using a rabbit polyclonal anti-DβH antiserum (1:1000; prod. no. sc-15318; Santa Cruz Biotechnology, Santa Cruz, CA), as described (Ibrahim and Briski, 2014; Briski and Shrestha, 2016; Alenazi et al., 2016). Protein molecular weight markers were included in each Western blot analysis.

Statistical analyses

Mean normalized protein O.D., NE, and plasma glucose, glucagon, and corticosterone measures were evaluated between treatment groups by two-way analysis of variance and Student Newman Keuls *post hoc* test. Differences of $p<0.05$ were considered significant.

RESULTS

Fig. 1 illustrates effects of intra-CV4 administration of the monocarboxylate transporter inhibitor 4CIN on VMN $GAD_{65/67}$ protein expression (Fig. 1A; $F_{(3,9)=}16.52$; $p<0.0001$) and NE content (Fig. 2B; $F_{(3,9)=}27.36$; $p=0.0001$) in animals that were pretreated by the neurotoxin 6OHDA *vs.* vehicle administration to the CV4. Data show that 6OHDA exposure significantly enhanced $GAD_{65/67}$ levels compared to V-pretreated controls (6OHDA/V *vs.* V/V) (Fig. 1A). This protein profile was also augmented by 4CIN (V/4CIN *vs.* V/V). Stimulatory effects of 4CIN on $GAD_{65/67}$ expression were abolished by 6OHDA (6OHDA/4CIN *vs.* 6OHDA/V). 6OHDA caused a significant reduction in VMN NE accumulation. VMN NE activity was amplified by 4CIN; this response was abolished by prior neurotoxin exposure.

Fig. 2 depicts effects of 6OHDA on expression levels of VMN GS (Fig. 2A; $F_{(3,9)=}4.80$; $p=0.03$) and the GP variants GPmm (Fig. 2B; $F_{(3,9)=}15.20$; $p=0.0002$) and GPbb (Fig. 2C; $F_{(3,9)=}47.15$; $p<0.0001$) following CV4 administration of 4CIN. As shown in Fig. 2A, 6OHDA elevated baseline VMN GS protein expression. 4CIN alone did not alter GS profiles, but this treatment reversed neurotoxin augmentation of GS content 6OHDA significantly inhibited VMN GPmm protein expression (Fig. 2B). This protein profile was also diminished after 4CIN administration to V-pretreated rats; this suppressive drug effect was abolished by 6OHDA pretreatment. The 6OHDA/V treatment group exhibited up-regulated VMN GPbb content (Fig. 2C). 4CIN administration significantly enhanced GPbb expression in both vehicle- and 6OHDA-pretreated groups.

Neurotoxin effects on DVC A2 area DβH protein content are shown in Fig. 3 ($F_{(3,9)}=9.09$; $p=0.0004$). Results indicate that DβH expression did not differ between 6OHDA/V and V/V treatment groups, but that 4CIN augmentation of this protein profile was prevented by neurotoxin pretreatment.

Effects of 6OHDA on plasma glucose (Fig. 4A; $F_{(3,12)=}5.20$; $p=0.03$), glucagon (Fig. 4B; $F_{(3,12)=}6.55$; $p=0.02$), and corticosterone (Fig. 4C; $F_{(3,12)=}18.80$; $p=0.0006$) responses to 4CIN are shown in Fig. 4. 6OHDA did not modify baseline circuiting glucose or counter-regulatory hormone concentrations. However, neurotoxin pretreatment abolished hindbrain lactoprivic stimulation of these plasma profiles.

DISCUSSION

Current research expanded upon recent evidence for exogenous NE regulation of VMN GPbb and $GAD_{65/67}$ protein expression (Mahmood et al., 2019) to investigate whether endogenous noradrenergic signaling is involved in physiological regulation of VMN glucose-regulatory and glycogen metabolic function. Outcomes demonstrate that homeostatic and lactoprivic patterns of DVC A2 noradrenergic signaling impose distinctive regulatory effects on VMN gluco-inhibitory GABAergic transmission and GP variant expression. Results show that pharmacological hindbrain lactoprivation elevates VMN NE activity relative to baseline. Metabolic status-dependent NE stimulus strength is correlated with differential adjustments in VMN $GAD_{65/67}$ and NE-sensitive GPmm expression; further effort is required to elucidate the

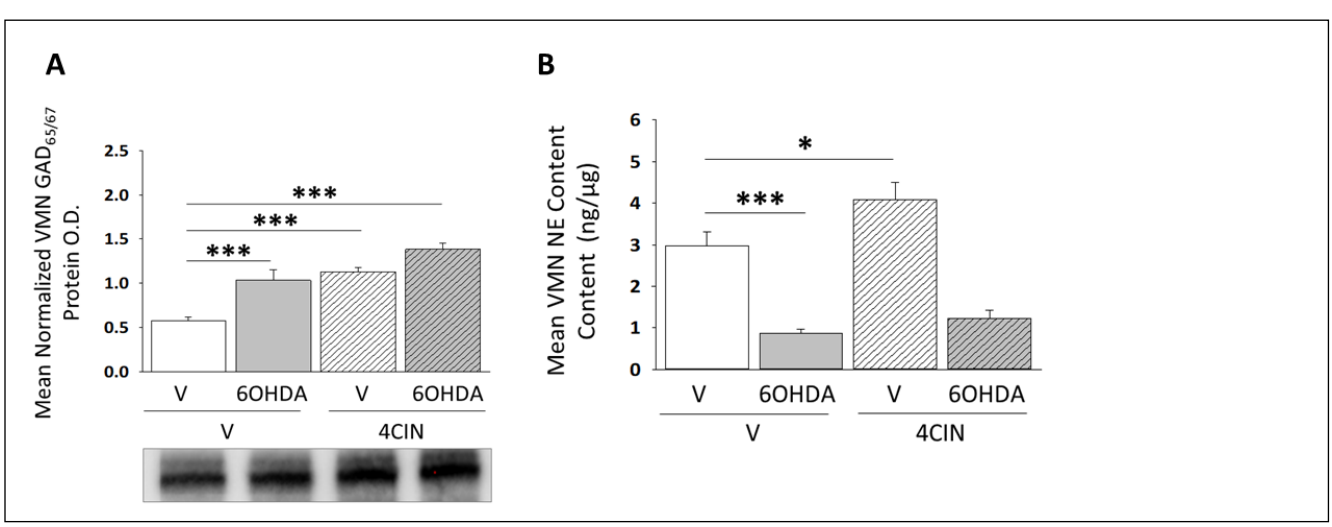

Fig. 1. Effects of pharmacological hindbrain lactoprivation on vmn glutamate decarboxylase$_{65/67}$ ($GAD_{65/67}$) protein expression and norepinephrine (NE) tissue content in vehicle (V) *vs.* 6OHDA-pretreated male rats. Data in Fig. 1A depict mean VMN $GAD_{65/67}$ O.D. measures + S.E.M. for V/V, 6OHDA/V, V/4CIN, and 6OHDA/4CIN treatment groups. Fig. 1B shows mean VMN NE tissue content ± S.E.M. for the same groups. *$p<0.05$; **$p<0.01$; ***$p<0.001$.

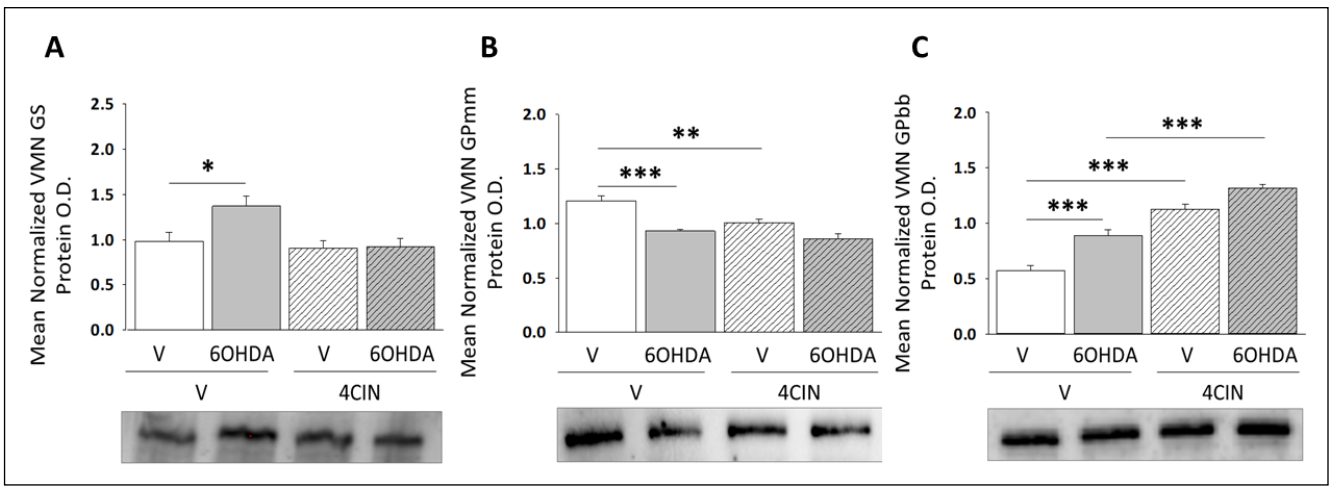

Fig. 2. Effects of precedent catecholaminergic neurotoxin exposure on ventromedial hypothalamic nucleus (VMN) glycogen metabolic enzyme protein responses to caudal fourth ventricular (CV4) administration of the monocarboxylate transporter inhibitor alpha-cyano-4-hydroxycinnamic acid (4CIN). Groups of male rats were injected into the CV4 with vehicle (V; groups 1 (n=4) and 3 (n=4) or the neurotoxin 6-hydroxydopamine (6OHDA; 75 ug/1.0 µL; groups 2 (n=4) and 4 (n=4) at -24 and -72 prior to t_o. At t_o, animals received intra-CV4 injections of V (groups 1 and 2) or 4CIN (75 ug/2.0 uL; groups 3 and 4). Micropunched VMN tissue was analyzed by Western blot for glycogen synthase (GS; Fig. 2A), glycogen phosphorylase-muscle type (GPmm; Fig. 2B), or glycogen phosphorylase-brain type (GPbb; Fig. 2C). Data depict mean normalized protein optical density (O.D.) measures ± S.E.M. for the following treatment groups: V/V (solid white bars); 6OHDA/V (solid gray bars); V/4CIN (diagonal-striped white bars); 6OHDA/4CIN (diagonal-striped gray bars). *p<0.05; **p<0.01; ***p<0.001.

mechanisms that may underlie bi-directional noradrenergic regulation of these proteins. Baseline NE input diminishes VMN energy-sensitive GPbb profiles, but lactoprivation augments this GP variant via catecholaminergic-independent cues. Inverse lactoprivic regulation of VMN GPmm and GPbb expression is presumed to facilitate energy deficit- as opposed to neurotransmitter-mediated control of local glycogen breakdown. Present observations that hindbrain lactoprivation elicits hyperglycemia and stimulates counter-regulatory hormone secretion affirm hindbrain metabolic sensor involvement in neural regulation of glucostasis.

Current findings provide novel evidence that DVC noradrenergic signaling may inhibit VMN GABAergic transmission during energy homeostasis. It remains to be determined if down-regulated GABA release diminishes local gluco-inhibitory tone during glucostasis, or alternatively, whether GABA suppression of counter-regulation is characteristic of states of metabolic dys-equilibrium. The latter scenario cannot be discounted as investigation of effects of pharmacological GABA receptor inhibition on counter-regulatory outflow has been performed in hypoglycemic, but not euglycemic rats (Chan et al., 2006; 2013). Present data show that 4CIN-induced hindbrain lactoprivation up-regulates VMN $GAD_{65/67}$ protein expression in male rats. Deterrence of this positive response to 4CIN by neurotoxin pretreatment implies that noradrenergic transmission is required for this drug action. Results provide original proof that hindbrain NE may exert bi-directional, signal strength (e.g., metabolic status) - dependent effects on VMN GABA transmission. The mechanisms that underlie these divergent effects of baseline *vs.* enhanced noradrenergic input on this gluco-regulatory neurotransmitter remain unclear.

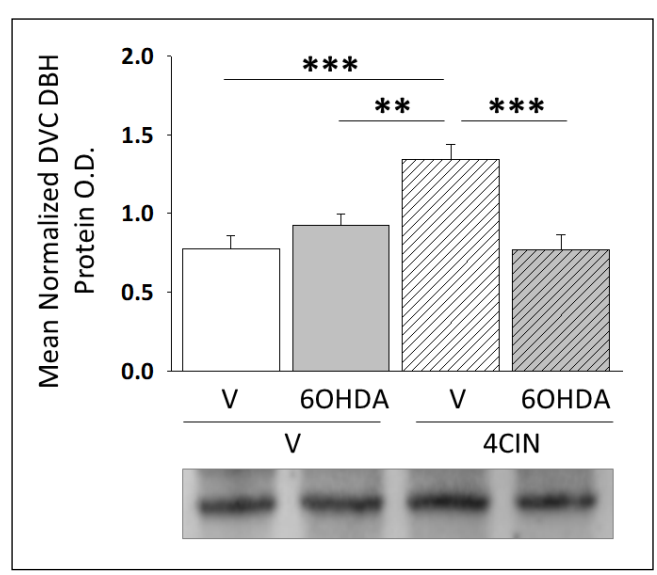

Fig. 3. Effects of 6OHDA pretreatment on dorsal vagal complex A2 cell area dopamine-beta-hydroxylase (DβH) protein expression in vehicle (V) *vs.* 4CIN-injected animals. Data depict mean normalized tissue DβH O.D. measures ± S.E.M. for V/V (solid white bars), 6OHDA/V (solid gray bars), V/4CIN (diagonal-striped white bars), and 6OHDA/4CIN (diagonal-striped gray bars) treatment groups. *p<0.05; **p<0.01; ***p<0.001.

Previous studies in our laboratory showed that in male rats, whole VMN $GAD_{65/67}$ profiles are, depending upon insulin dosage, either refractory to (Mahmood et al., 2018; 10.0 U neutral protamine Hagedorn insulin (NPH)/kg bw, sc) or decreased (Mandal and Briski, 2018; 5.0 U NPH/kg bw, sc) in response to the systemic metabolic stress of bolus insulin injection-induced hypoglycemia. It should be noted that disparate outcomes from prior *vs.* current work credibly point toward differences between experimental models, including pharmacological activation of a single metabolic sensory cell population, e.g., hindbrain A2 neurons, *vs.* hypoglycemia-associated body-wide sensor activation. Under the latter circumstances, noradrenergic stimulation of $GAD_{65/67}$ expression may be attenuated by neurotransmitter cues provided by other energy sensors to the VMN. In light of evidence that direction of change in VMN NE activity in hypoglycemic animals depends upon NPH dosage (Alhamami et al., 2018), it is possible that magnitude of metabolic deficit-driven NE input to the VMN may be a critical determinant to GABA response to hypoglycemia.

Work involving astrocyte cell culture models bolsters the novel concept that brain GP variants exhibit differential reactivity to distinctive physiological stimuli, thereby endowing discriminative glycogen reactivity to specific regulatory signals (Müller et al., 2015). Data here document divergent effects of basal and lactoprivic NE signaling on VMN GPmm versus GPbb protein expression *in vivo*. 6OHDA-induced augmentation of GPbb alongside inhibition of GPmm profiles in non-4CIN – treated rats indicates that VMN energy-sensitive GPbb expression is suppressed by basal noradrenergic input, whereas NE-sensitive GPmm is enhanced by the same signal. 4CIN elevated VMN GPbb, but inhibited GPmm protein, implying that hindbrain lactoprivation stimulates GPbb while decreasing GPmm protein levels in that structure. Neurotoxin pretreatment did not prevent 4CIN augmentation of GPbb, but blocked drug suppression of GPmm. Results indicate that increasing NE input from basal to lactoprivic levels changes the direction of regulatory effect, e.g., stimulatory to inhibitory, on GPmm. NE-mediated suppression of the NE-responsive GP variant may have the effect of sparing glycogen mobilization in the absence of VMN energy deficiency. At the same time, hindbrain lactoprivation augmented VMN levels of the energy-sensitive GP variant GPbb, an outcome that is presumed to facilitate glycogen breakdown when energy is insufficient. It is notable that lactoprivation up-regulates GPbb via non-noradrenergic mechanisms, an action that could involve lactoprivic patterns of A2 nerve cell release of co-expressed non-catecholaminergic transmitters or, alternatively, signaling by lactoprivic-sensitive non-catecholaminergic hindbrain neurons. Further research is needed to compare rates and magnitude of VMN glycogen mobilization in response to homeostatic versus hypoglycemic patterns of hindbrain NE input, and to determine if lactoprivic cues from the hindbrain are a major determinant of glycogen dissolution during hypoglycemia. Additional work is required to investigate the mechanisms that mediate bi-directional effects of baseline versus lactoprivic hindbrain signaling on VMN GPmm expression. In light of evidence that NE regulates VMN astrocyte α_2 and β_1 AR protein profiles (Ibrahim et al., 2019), it is speculative that effects of distinctive NE stimulus strength on this GP variant may involve, in part, adjustments in ratio of expressed AR proteins and corresponding changes in post-receptor signal transduction.

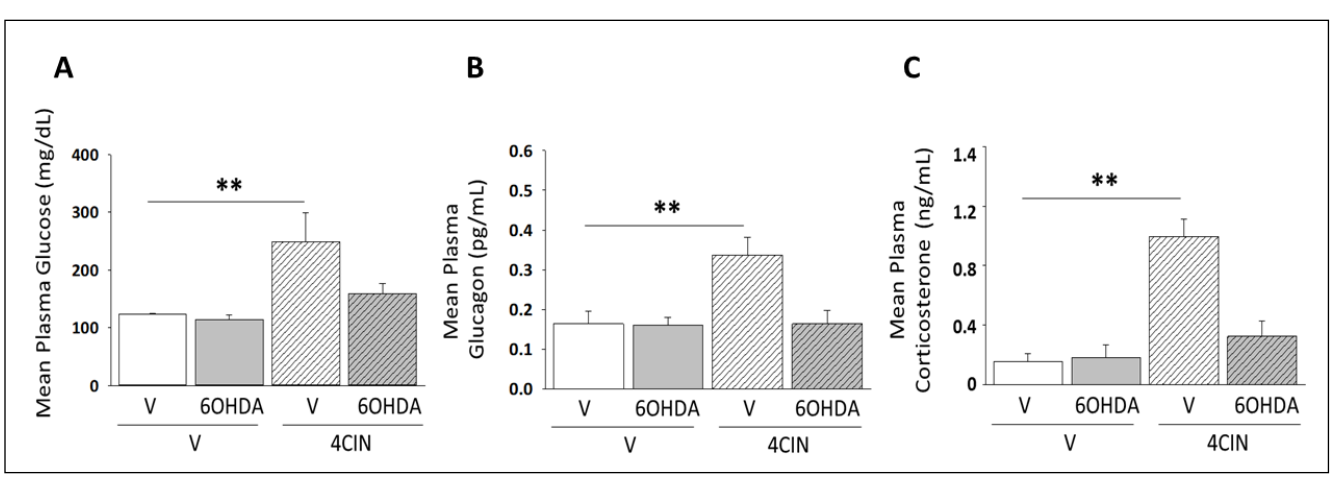

Fig. 4. Hindbrain lactoprivic regulation of plasma glucose and counter-regulatory hormone concentrations; impact of 6OHDA pretreatment. Mean plasma glucose (Fig. 4A), glucagon (Fig. 4B), and corticosterone (Fig. 4C) levels ± S.E.M. are presented for V/V, 6OHDA/V, V/4CIN, and 6OHDA/4CIN treatment groups. *p<0.05; **p<0.01; ***p<0.001.

Earlier research documented parallel up-regulation of GPbb and $GAD_{65/67}$ by intra-VMN administration of NE, and reliance of this positive $GAD_{65/67}$ response to NE on astrocyte substrate fuel provision (Mahmood et al., 2019). Here, homeostatic patterns of hindbrain NE input to the VMN were inhibitory to both GPbb and $GAD_{65/67}$, whereas lactoprivic-driven NE noradrenergic signaling, which was elevated above baseline, stimulated $GAD_{65/67}$ but not GPbb expression. It might be that greater increments in magnitude of NE activity are required to enhance this GP variant. At the same time, GPmm and $GAD_{65/67}$ expression patterns underwent inverse adjustments in response to 6OHDA or 4CIN, via NE-dependent mechanisms. These findings do not constitute definitive proof of a causal relationship between one or both GP variants and $GAD_{65/67}$, but emphasize the need for further effort to explore this possibility.

Observations here of significant diminution of baseline VMN tissue NE content in 6OHDA – treated rats affirm that DVC A2 neurons are a principal source of noradrenergic innervation to that structure during energy homeostasis. Data also show that 4CIN increased VMN NE activity and that this response was prevented by 6OHDA. In earlier studies involving a lesser dosage of 4CIN, a net reduction in VMN NE content was detected at +2 h (Briski and Mandal, 2019), the time point utilized here. As 4CIN elicits dose-proportionate Fos expression in multiple hypothalamic gluco-regulatory loci, including the VMN (Briski and Patil, 2005), we presume that noradrenergic lactoprivic signaling may likely increase corresponding to drug dosage strength. Since the lower 4CIN dose suppressed VMN $GAD_{65/67}$ and GPmm profiles (responses similar to outcomes described here), it is likely reductions in NE content observed at +2 h after administration of that dosage succeeded an earlier elevation in NE activity in that site. Here, prevention of 4CIN-induced increases in VMN NE accumulation by 6OHDA verifies that DVC A2 cells respond to lactoprivation by enhancing NE transmission to the VMN.

Our previous work demonstrated that the 6OHDA protocol used here consistently causes significant diminution of numbers of tyrosine hydroxylase-immunopositive neurons in the DVC A2 area (Gujar et al., 2014; Tamrakar et al., 2015; Alhamami et al., 2018). As immunocytochemical data do not shed light on residual activity of surviving A2 neurons, Western blot analysis of the rate-limiting catecholamine biosynthetic enzyme DβH expression was performed here to assess basal and 4CIN-associated patterns of noradrenergic signaling after neurotoxin exposure. Although 6OHDA was predicted to decrease A2 area tissue DβH levels, current results show that mean protein content did not differ between neurotoxin- versus vehicle-pretreated groups. However, lactoprivic intensification of DβH expression was prevented by 6OHDA pretreatment. These outcomes suggest that neurotoxin-resilient A2 neurons may up-regulate this protein profile as an adaptive response to reductions in cell population size. Yet, 6OHDA-associated suppression of VMN NE accumulation in vehicle- and 4CIN-treated animals implies that baseline and stimulus-induced neurotransmission by surviving A2 nerve cells is significantly impaired.

Results show that 6OHDA did not modify baseline plasma glucose, glucagon, or corticosterone concentrations, but did prevent 4CIN augmentation of circulating glucose and counter-regulatory hormone levels. These data imply that during energy stability, baseline hindbrain noradrenergic input may be one of several parallel, redundant cues that regulate glucostasis, so that that silencing of this specific signal does not significantly alter blood glucose levels. Yet, augmented NE transmission due to lactoprivation is correlated with elevated plasma glucose, glucagon, and corticosterone levels, outcomes previous reported by our laboratory (Gujar et al., 2014), findings confirm that prior reports that hindbrain lactate status has a critical impact on shaping glycemic responses to insulin administration (Patil and Briski, 2005). Coincident drug-induced hyperglycemia and up-regulated counter-regulatory hormone secretion supports the likelihood that the former may tamper the latter responses.

In summary, current research documents differential effects of homeostatic versus lactoprivic, e.g., augmented VMN NE activity patterns on VMN gluco-inhibitory GABAergic transmission and GP variant expression. Additional work will be necessary to identify mechanisms that mediate physiological bi-directional noradrenergic regulation of these proteins. Baseline NE input was observed to elevate VMN NE-sensitive GPmm and suppress energy-sensitive GPbb profiles, but the latter protein was up-regulated during hindbrain lactoprivation by NE-independent cues. Opposing effects of hindbrain lactoprivation on VMN GPmm and GPbb expression may promote facilitate energy deficit- *vs.* neurotransmitter-regulation of glycogen disassembly in that site. Present evidence that hindbrain lactoprivation causes hyperglycemia and increases counter-regulatory hormone secretion bolsters hindbrain metabolic sensor involvement in neural regulation of glucostasis. Further studies are needed to examine whether lactoprivic augmentation of VMN GABA signaling reflects GABA neuron metabolic stability due to NE-dependent (e.g., direct noradrenergic input to these neurons) as well as NE-independent, e.g., GPbb-mediated glycogen liberation of oxidizable substrate fuel.

REFERENCES

Alenazi FSH, Ibrahim BA, Al-Hamami H, Shakiya M, Briski KP (2016) Role of estradiol in intrinsic hindbrain AMPK regulation of hypothalamic AMPK, metabolic neuropeptide, and norepinephrine activity and food intake in the female rat. Neuroscience 314: 35–46.

Alhamami HN, Uddin MM, Mahmood ASMH, Briski KP (2018) Lateral but not medial hypothalamic AMPK activation occurs at the hypoglycemic nadir in insulin-injected male rats: Impact of caudal dorsomedial hindbrain catecholamine signaling. Neuroscience 379: 103–114.

Ali MH, Napit PR, Mahmood ASMH, Bheemanapally K, Alhamami HN, Uddin MM, Mandal KS, Ibrahim MMH, Briski KP (2019) Hindbrain estrogen receptor regulation of ventromedial hypothalamic glycogen metabolism and glucoregulatory transmitter expression in the hypoglycemic male rat. Neuroscience 409: 253–260.

Bélanger M, Allaman I, Magistretti PJ (2011) Brain energy metabolism: focus on astrocyte-neuron metabolic cooperation. Cell Metab 14: 724–738.

Beverly JL, de Vries, MG, Beverly MF, Arseneau LM (2000) Norepinephrine mediates glucoprivic-induced increase in GABA in the ventromedial hypothalamus of rats. Amer J Physiol Regul Integr Comp Physiol 279: R990-R996.

Beverly JL, De Vries MG, Bouman SD, Arseneau LM (2001) Noradrenergic and GABAergic systems in the medial hypothalamus are activated during hypoglycemia. Amer J Physiol Regul Integr Comp Physiol 280: R563–569.

Borg MA, Sherwin RS, Borg WP, Tamborlane WV, Shulman GI (1997) Local ventromedial hypothalamus glucose perfusion blocks counterregulation during systemic hypoglycemia in awake rats. J Clin Invest 99: 361–365.

Borg MA, Tamborlane WV, Shulman GI, Sherwin RS (2003) Local lactate perfusion of the ventromedial hypothalamus suppresses hypoglycemic counterregulation. Diabetes 52: 663–666.

Briski KP, Mandal SK (2019) Hindbrain lactoprivic regulation of hypothalamic neuron transactivation and glucoregulatory neurotransmitter expression: Impact of antecedent insulin-induced hypoglycemia. Neuropeptides 77: 101962.

Briski KP, Koshy Cherian A, Genabai NK, Vavaiya KV (2009) *In situ* coexpression of glucose and monocarboxylate transporter mRNAs in metabolic-sensitive dorsal vagal complex catecholaminergic neurons: transcriptional reactivity to insulin-induced hypoglycemia and caudal hindbrain glucose or lactate repletion during insulin-induced hypoglycemia. Neuroscience 164: 1152–1160.

Briski KP, Patil GD (2008) Induction of Fos immunoreactivity labeling in forebrain metabolic loci by caudal fourth ventricular administration of the monocarboxyate transporter inhibitor, α-cyano-4-hydroxycinnamic acid. Neuroendocrinology 82: 49–57.

Briski KP, Shrestha PK (2016) Hindbrain estrogen receptor-beta antagonism normalizes reproductive and counter-regulatory hormone secretion in hypoglycemic steroid-primed ovariectomized female rats. Neuroscience 331: 62–71.

Brown AM (2004) Brain glycogen re-awakened. J Neurochem 89: 537–552.

Chan O, Paranjape SA, Horblitt A, Zhu W, Sherwin RS (2013) Lactate-induced release of GABA in the ventromedial hypothalamus contributes to counterregulatory failure in recurrent hypoglycemia and diabetes. Diabetes 62: 4239–4246.

Chan O, Zhu W, Ding Y, McCrimmon RJ, Sherwin RS (2006) Blockade of GABA(A) receptors in the ventromedial hypothalamus further stimulates glucagon and sympathoadrenal but not the hypothalamo-pituitary-adrenal response to hypoglycemia. Diabetes 55: 1080–1087.

Cherian A, Briski KP (2011) Quantitative RT PCR and immunoblot analyses reveal acclimated A2 noradrenergic neuron substrate fuel transporter, glucokinase, phospho-AMPK, and dopamine-beta-hydroxylase responses to hypoglycemia. J Neurosci Res 89: 1114–1124.

Dong JH, Chen X, Cui M, Yu X, Pang Q, Sun JP (2012) B2-adrenergic receptor and astrocyte glucose metabolism. J Mol Neurosci 48: 456–463.

Donovan CM, Watts AG (2014) Peripheral and central glucose sensing in hypoglycemic detection. Physiology 29: 314–324.

Fillenz M, Lowry JP, Boutelle MG, Fray AE (1999) The role of astrocytes and noradrenaline in neuronal glucose metabolism. Acta Physiol Scand 167: 275–284.

Gruetter R (2003) Glycogen: the forgotten cerebral energy store. J Neurosci Res 74: 179–183.

Gujar AD, Ibrahim BA, Tamrakar P, Briski KP (2013) Hypoglycemia differentially regulates hypothalamic glucoregulatory neurotransmitter gene and protein expression: Role of caudal dorsomedial hindbrain catecholaminergic input. Neuropeptides 47: 139–147.

Gujar AD, Ibrahim BA, Tamrakar P, Koshy Cherian A, Briski KP (2014) Hindbrain lactostasis regulates hypothalamic AMPK activity and hypothalamic metabolic neurotransmitter mRNA and protein responses to hypoglycemia. Amer J Physiol Regul Integ Comp Physiol 306: R457-R469.

Ibrahim BA, Briski KP (2014) Role of dorsal vagal complex A2 noradrenergic neurons in hindbrain glucoprivic inhibition of the luteinizing hormone surge in the steroid-primed ovariectomized female rat: Effects of 5-thioglucose on A2 functional biomarker and AMPK activity. Neuroscience 269: 199–214.

Ibrahim MMH, Alhamami HN, Briski KP (2019) Norepinephrine regulation of ventromedial hypothalamic nucleus metabolic transmitter biomarker and astrocyte enzyme and receptor expression: role of 5′-AMP-activated protein kinase. Brain Research 1711: 48–57.

Magistretti PJ, Sorg O, Yu N, Martin JL, Pellerin L (1993) Neurotransmitters regulate energy metabolism in astrocytes: implications for the metabolic trafficking between neural cells. Dev Neurosci 15: 306–312.

Mahmood ASMH, Bheemanapally K, Mandal SK, Ibrahim MMH, Briski KP (2019) Norepinephrine control of ventromedial hypothalamic nucleus glucoregulatory neurotransmitter expression in the female rat: role of monocarboxylate transporter function. Mol Cell Neurosci 95: 51–58.

Mandal SK, Briski KP (2018) Hindbrain dorsal vagal complex AMPK controls hypothalamic AMPK activation and metabolic neurotransmitter protein expression and counter-regulatory hormone secretion in the hypoglycemic male rat. Brain Res Bull 144: 171–179.

Müller MS, Pedersen SE, Walls AB, Waagepetersen HS, Bak LK (2015) Isoform-selective regulation of glycogen phosphorylase by energy deprivation and phosphorylation in astrocytes. Glia 63: 154–162.

Nadeau OW, Fontes JD, Carlson GM (2018) The regulation of glycogenolysis in the brain. J Biol Chem 293: 7099–7109.

Napit PR, Ali MH, Shakya M, Mandal SK, Bheemanapally K, Mahmood ASMH, Ibrahim MMH, Briski KP (2019) Hindbrain estrogen receptor regulation of counter-regulatory hormone secretion and ventromedial hypothalamic nucleus glycogen content and glucoregulatory transmitter signaling in hypoglycemic female rats. Neuroscience 411: 211–221.

Oomura Y, Ono H, Ooyama H, Wayner MJ (1969) Glucose and osmosensitive neurons of the rat hypothalamus. Nature 222: 282–284.

Patil GD, Briski KP (2005) Lactate is a critical 'sensed' variable in caudal hindbrain monitoring of CNS metabolic stasis. Amer J Physiol Regul Integr Physiol 289: R1777–1786.

Pellerin L, Pellegri G, Bittar PG, Charnay Y, Bouras C, Martin JL (1998) Evidence supporting the existence of an activity-dependent astrocyte-neuron lactate shuttle. Dev Neurosci 20: 291–299.

Shakya M, Shrestha PK, Briski KP (2018) Hindbrain 5′-monophosphate-activated protein kinase mediates short-term food deprivation inhibition of the gonadotropin-releasing hormone-luteinizing hormone axis: role of nitric oxide. Neuroscience 383: 46–59.

Shrestha PK, Tamrakar P, Ibrahim BA, Briski KP (2014) Hindbrain medulla catecholamine cell group involvement in lactate-sensitive hypoglyce-

mia-associated patterns of hypothalamic norepinephrine and epinephrine activity. Neuroscience 278: 20–30.
Silver IA, Erecińska M (1998) Glucose-induced intracellular ion changes in sugar-sensitive hypothalamic neurons. J Neurophysiol 79: 1733–1745.
Stobart JL, Anderson CM (2013) Role of astrocytes as gatekeepers of neuronal energy supply. Front Cell Neurosci 7: 1–21.
Tamrakar P, Shrestha PK, Briski KP (2015) Dorsomedial hindbrain catecholamine regulation of hypothalamic astrocyte glycogen metabolic enzyme protein expression: Impact of estradiol. Neuroscience 292: 34–45.
Watts AG, Donovan CM (2010) Sweet talk in the brain: glucosensing, neural networks, and hypoglycemic counterregulation. Front Neuroendocrinol 31: 32–43.